Int. J. Electrochem. Sci., 8 **(2013)** 5382 - 5395

International Journal of
ELECTROCHEMICAL
SCIENCE
www.electrochemsci.org

Preparation and Characterization of PbO_2 Electrodes Doped with TiO_2 and Its Degradation Effect on Azo Dye Wastewater

Hao Xu[1,2], *Qian Zhang*[1], *Wei Yan*[1,*] , *Wei Chu*[2], *Longfei Zhang*[1]

[1]Department of Environmental Science and Engineering, Xi'an Jiaotong University, Xi'an 710049, China
[2]Department of Civil and Environmetal Engineering, The Hong Kong Polytechnic Univerisity, Hung Hom, Kowloon, Hong Kong
[*]E-mail: yanwei@mail.xjtu.edu.cn

Received: 10 December 2012 / *Accepted:* 16 February 2013 / *Published:* 1 April 2013

In this paper, P25-TiO_2 doped PbO_2 electrodes based on the Ti/SnO_2-Sb substrate were prepared by the co-deposition method. The XRD results justified that P25 particles have been successfully doped into the PbO_2 layer. The surface morphology of prepared electrodes was examined by scanning electron microscopy. It was found that the doped PbO_2 electrode has a more compact and dense surface with no flaw or crack on it, comparing to those of undoped electrodes. The accelerated life test demonstrated that the doped PbO_2 electrode has a better stability than the undoped one. A significant synergetic effect was observed in the organic degradation test under illumination using the doped PbO_2 electrode, as evidenced by linear scanning voltammetry. Acidic condition (pH < 7) induces a better performance in methyl orange degradation due to a higher adsorption of methyl orange on the TiO_2 surface. All the doped electrodes with different TiO_2 doping levels presented high removal efficiency under irradiation, though the increase in service lifetime was not observed. A TiO_2 doping amount of 5 $g \cdot L^{-1}$ is established as the optimal dosage for preparing the electrode for the higher performance in both the accelerated life and the degradation tests.

Keywords: PbO_2, TiO_2; photoelectroanode, photo-electrochemical catalysis, synergetic effect

1. INTRODUCTION

Azo dyes are typical organic pollutants found in effluent of many printing industries. Due to its refractory traits of deep color, high chemical oxygen demand (COD) and low biodegradability, severe environmental problems are triggered[1]. Many attempts have been made to deal with this issue including advanced oxidation technology, electrochemical oxidation[1-4] and photochemical oxidation[5-7], attributed to their excellent performance in organic removal. However, many problems are still yet to be resolved[8, 9].

For photochemical oxidation technique, one of the main problems is the rapid recombination of photo-generated electrons and holes, which restrains the improvement in treatment efficiency[10, 11]. Another obstacle in practical applications lies with the recovery of photocatalysts from heterogeneous phase. Hence any approach that can lower the recombination rate and minimize the need in recovery of photocatalytic particles would be of great benefit[10]. To enhance the photocatalytic activity in degradation of organic pollutants, electrochemical oxidation is proposed to combine with photocatalysis to exhibit a synergetic effect during the treatment[12-15]. Specifically speaking, photocatalytic particles are immobilized on electrodes with uniform dispersion to form photoelectroanodes. Meanwhile, photogenerated carriers are effectively separated through the driving force of applied bias between the electrodes. In this way, the drawbacks of photochemical oxidation approach can be reduced or eliminated.

Referring to electrochemical oxidation method, highly efficient treatment relies on the choice of anode materials. In general, high corrosion resistances and physiochemical stability under high positive potentials are priority. PbO_2 has been regarded as an excellent metal oxide material in terms of the characteristics mentioned above[16]. Moreover, the relatively cheap price compared with noble metals and good conductivity also motivates scientists to perform extensive research on it. PbO_2 electrodes were conventionally fabricated by electrodepositing Pb^{2+} on the pretreated Ti substrate with an intermediate layer of Sb-doped SnO_2[17, 18]. The preparation process is relatively simple and easy to control the electrodes' property. However, the conventional Ti/PbO_2 electrode has two disadvantages: (1) the service lifetime of Ti/PbO_2 coating is quite limited due to the strong inner stress[19]; (2) the Ti/PbO_2 electrodes can easily degrade large organic molecules into small ones, but is difficult for a complete mineralization of these small molecules[20-22]. Thus, better electrodes targeting on organic pollutant degradation are desired. P25-TiO_2 is a widely used photocatalyst with its superior photocatalytic activity attributed to anatase/rutile which facilitates the separation of photogenerated electrons and holes. Li[14, 23-25] et al. has reported that a significant synergetic effect of photoelectrocatalysis was observed on the TiO_2 modified $Ti/Ru_{0.3}Ti_{0.7}O_2/PbO_2$ electrode. In this study, P25-TiO_2 was doped into the PbO_2 layer through electrochemical deposition, which further enhanced the photoelectrocatalytic performance of the PbO_2 electrodes. In addition, it was assumed that the service life of the newly prepared electrode could be greatly enhanced through co-deposition, because TiO_2 particles doped in the PbO_2 layer can improve compactness of the original Ti/PbO_2 electrode and reduce the inner stress of the PbO_2 layer. The purpose of this work is to assess the photoelectrocatalytic activity of P25-TiO_2 doped Ti/PbO_2 electrodes in degradation of organic wastewater. Methyl orange (MO), a typical azo dye, was chosen as the probe in the degradation process.

2. METHODOLOGY

2.1 Electrode preparation

High purity of titanium (Ti) foil (99.6%) with 0.5mm-thickness was used (BaoTi Co. Ltd, China) in this study. All the water was deionized water produced from an EPET-40TF system (EPET Co. Ltd, Nanjing, China).

Prior to the electrode preparation process, Ti plates with a dimension of 3cm×3cm were mechanically polished with 1000-grid abrasive papers, and then rinsed with deionized water. The foils were subsequently immersed into a mixture of acetone and 1 $mol \cdot L^{-1}$ NaOH (1:1 v/v) in an ultrasonic bath (KQ2200DB, 80W, 40 KHz, Kunshan Ultra Co. Ltd, Jiangsu, China) for removing organic residues from the surface, and followed by etching in 10 wt% oxalic acid at 98℃ for 2h, then the products were rinsed thoroughly with deionized water.

The Ti/Sb-SnO_2/PbO_2 electrode was prepared via two steps: (1) deposit the inner coating layer (Sb-SnO_2) through thermal decomposition; (2) electrochemical deposition of the outer layer of PbO_2. In the first step, the precursor solution was composed of $SnCl_4 \cdot 6H_2O$ and $SbCl_3$ dissolved in a mixed solution made up of *n*-butanol, *iso*-propanol, ethanol and hydrochloric acid (37%). The salts were mixed in stoichiometric amounts according to the desired nominal composition. It should be noted that the precursor solution has to be freshly prepared and used for its poor stability. The titanium surface was brushed with the precursor solution, and subsequently calcined in an oven at 450°C for 15min, for the thermal deposition of expected metal oxide. This procedure was repeated for 10 times with a final annealing step at 450°C for an hour. At this moment, the surface of the titanium substrate has been covered by the blue-gray Sb-doped SnO_2 oxide. The average oxide loading for the dip coating method is 1.10 $mg \cdot cm^{-2}$, which is a typical value to ensure an appropriate service life of electrodes.

In the second step, the PbO_2 layer was coated on the as-prepared Ti/Sb-SnO_2 electrode through electrochemical deposition. By doing this, the interface resistance between the substrate and PbO_2 can be lessened. The electrochemical deposition process was carried out at 10 $mAcm^{-1}$ for 120min in a 65°C water bath, and powered by an DC source (WYK-303B, China).The electrolyte was composed of 0.5 $mol \cdot L^{-1}$ $Pb(NO_3)_2$, 0.1 $mol \cdot L^{-1}$ $Cu(NO_3)_2$, 0.01 $mol \cdot L^{-1}$ NaF, and 10 $mg \cdot dm^{-3}$ dodecyl sodium sulfonate (pH adjusted to 2 using HNO_3). Finally, the as-prepared Ti/Sb-SnO_2/PbO_2 electrode was rinsed by doubly-distilled water. For the P25 TiO_2 doped Ti/Sb-SnO_2/PbO_2 electrode, 5 $g \cdot L^{-1}$ of TiO_2 powder was added into the electrolyte during the electrochemical deposition process as mentioned above.

2.2 Electrode characterization and electrochemical measurement

The crystal structure of the as-prepared electrodes was characterized by a Rigaku D/MAX-2400X X-Ray Diffractometer with Cu-Ka radiation. The element content of the electrode was characterized by a X-Ray Fluorescence Spectrometer (XRF, S4 PIONEER, Bruker). The morphology of the metal oxide coating film was examined by SEM (JEOL, JSM-6390A).

The electrochemical characteristics of the electrodes were tested in a conventionally three-electrode cell at room temperature, with the as-prepared electrode served as the working electrode, Pt sheet as the counter electrode, and an Ag/AgCl/saturated KCl electrode as the reference electrode. The electrochemical measurement was conducted on an electrochemical system (LK3200A, Lanlike, China). For the accelerated life test, the current density was increased to 1500 $mA \cdot cm^{-2}$ in a 3 $mol \cdot L^{-1}$ H_2SO_4 solution at 40~45°C. The linear scanning voltammetry was carried out from 0.0 to 2.0 V versus Ag/AgCl/saturated KCl electrode at a scan rate of 50 $mV \cdot s^{-1}$, using a 20 $g \cdot L^{-1}$ Na_2SO_4 solution. The

chronoamperometry experiment was employed to test the photoeletroresponse of the TiO_2 doped PbO_2 electrode in a 20 $g \cdot L^{-1}$ Na_2SO_4 solution at constant potentials of 0.5 and 1.5V.

2.3 Probe degradation

All the degradation experiments were carried out in the three-electrode system. In combination with the working electrode (5 cm^2), a copper foil with the same working area was used as the cathode. The distance between the two electrodes was 2.0 cm with the active layer of the as-prepared anode facing to the quartz window. In the degradation process, the stirring and cooling systems were turned on immediately after 250ml methyl orange solution (50 $mg \cdot L^{-1}$) was added into the plexiglass reactor. In particular for the photoelectrodegradation process, the light source (CHF-XM-500W, Trusttech Co Ltd., Beijing, China) was turned on before the degradation process began. The electro-catalysis process and the photo/electro-catalysis process were both carried out under a constant potential (supported by LK3200A, Lanlike, China) for 2h. During the process, water samples were withdrawn at a time interval of 20 min for the UV-vis analyses (Agilent 8453). The removal efficiency was calculated according to the following formula:

$$\text{removal efficiency} = \frac{A_0 - A_t}{A_0} \times 100\% \qquad (1)$$

where A_0 and A_t are the absorbances of the solution at 465 nm for time zero and any given time t, respectively.

3. RESULTS AND DISCUSSION

3.1 XRD analysis

The XRD spectrum of the P25 TiO_2, undoped PbO_2 electrode and P25 TiO_2 doped PbO_2 electrode are shown in Fig. 1. For the P25 TiO_2 sample, it can be observed that the main diffraction peak at 25.3° corresponding to the (101) crystal face of anntase TiO_2 appears. For the undoped PbO_2 electrode, two types of PbO_2 crystallites can be distinguished by the main diffraction peaks at 32.0° and 62.5° that correspond to the (101) and (301) crystal surfaces of β-PbO_2 , where the diffraction peak at 36.0° corresponds to the (200) crystal surface of α-PbO_2. In addition, no diffraction peak at 25.3° is observed for undoped PbO_2 electrode. For the TiO_2 doped PbO_2 electrode, the main diffraction peaks at 25.3°, 32.2°, 36.1° and 49.0° are intensified. Compared with P25 and the undoped electrode, the diffraction peak at 25.3° for the doped electrode is sharp and strong, indicating that P25 particles were successfully doped into the PbO_2 layer. In the doped PbO_2 electrode, the peak at 49.0° is a new diffraction peak, while the diffraction peaks around 32° and 36° is red-shifted and the diffraction peak at 62.5° disappears. The XRD spectra results suggest that there were adsorption and embedding

processes involved during the co-deposition of P25 and PbO_2 layer. Thus, the co-deposition affected the growth of PbO_2 and changed its growth orientation, resulting in a change of its crystal face.

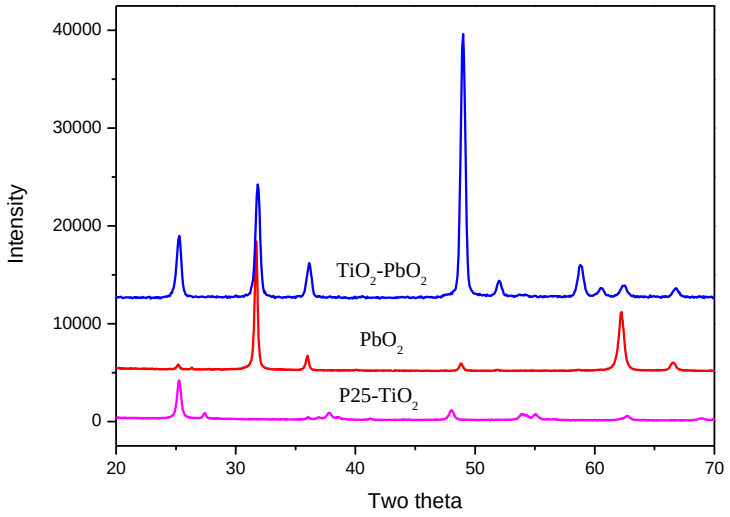

Figure 1. XRD patterns of the different samples

3.2 Surface morphology

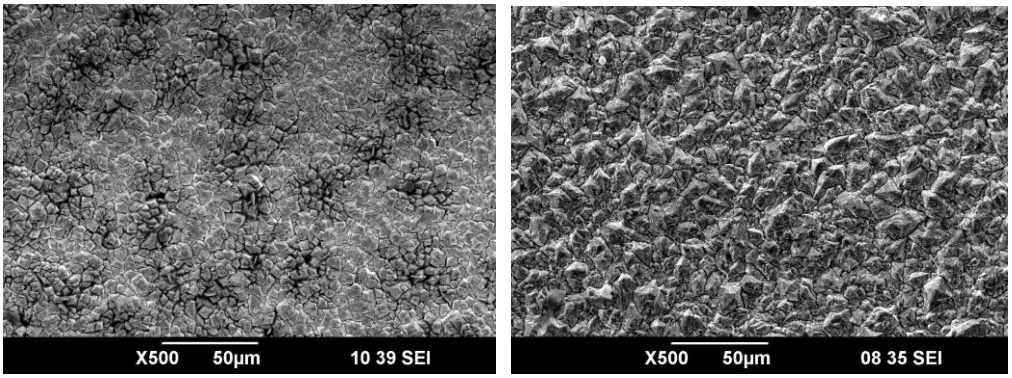

(a) (b)

Figure 2. SEM images for (a) undoped PbO_2 electrode and (b) P25-doped PbO_2 electrode

The morphology of the prepared electrodes was investigated by SEM as shown in Fig. 2. It was observed that the electrode surface changed significantly with the addition of TiO_2. Both electrodes have non-uniform texture which provided more surface area, increased the electrode efficiency and potentially exhibited a favorable advantage for the application of wastewater treatment. The crystal shape of the undoped PbO_2 electrode was quadrangular as shown in Fig. 2(a). There are considerable fractions of areas (i.e. black spots) that are not fully covered by PbO_2. It is presumed that cracks between these particles may lead to the chemical instability of electrodes in real applications. For the doped electrode, however, no apparent defects or cracks can be found on the surface. It is believed that

the doped PbO_2 electrode would have a longer service lifetime because the uncracked surface minimizes the diffusion of electrolytes into the titanium base.

3.3 Accelerated life test

In general, the use of common PbO_2 electrodes in the application of wastewater treatment is often limited because the evolution of oxygen on the anode that usually results in a relatively short electrode service life. The accelerated life tests of the electrodes prepared in this work were conducted to compare their electrochemical stability. A harsh condition using 3 $mol \cdot L^{-1}$ H_2SO_4 solution at a current density of 1500 $mA \cdot cm^{-2}$ was chosen to determine the lifetime of electrodes. The temperature of the sulfuric acid solution was kept at 45°C mainly due to the ohmic heating. Fig. 3 shows the potential changes with time by employing two electrodes. For the undoped PbO_2 electrode, a platform period with potential around 4.0 V ~5.0 V was observed, indicating the potential is relatively stable and the consumption of PbO_2 layer is fairly even. When the coating on the titanium base is worn out, a rapid increase of potential would be observed and it can be recognized as the deactivation of electrode. Similar pattern was also observed for the doped electrode. If 10 V (vs Ag/AgCl) was set as the deactivated criteria of electrodes, the service life of the doped electrode is 158 h, which is nearly 1.6 times longer than that of the undoped electrode (100.5h). Yao *et. al.* [26] used ZrO_2 nanoparticles to dope PbO_2 electrode and the service life of the PbO_2-ZrO_2 electrode was 148 h, which was shorter than the present work.

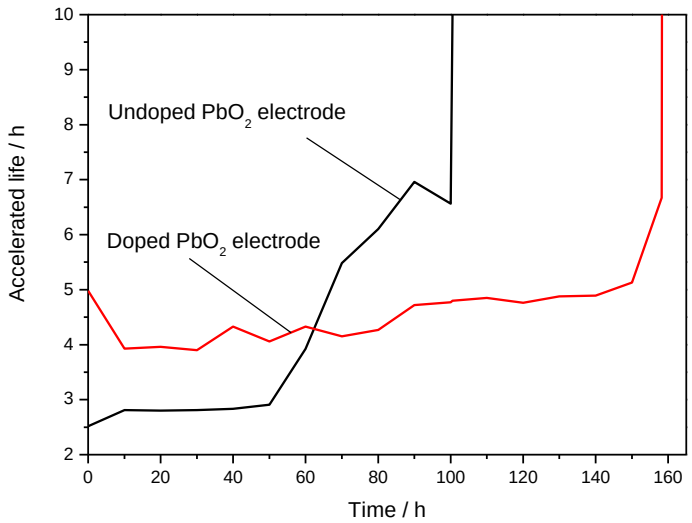

Figure 3. Accelerated life test of un-doped and doped PbO_2 electrodes in a 3 $mol \cdot L^{-1}$ H_2SO_4 solution under curent density of 1500 $mA \cdot cm^{-2}$

The stability of electrodes is affected by a variety of external factors, such as current density and electrolyte properties (acidity, salinity and temperature). Under the same external conditions, the electrode life depends on the characteristics of the electrode itself, such as the electrode surface oxide

deposition, the surface state density and stress level. In this work, The PbO_2 oxide loading was calculated to be 99 $mg \cdot cm^{-2}$ and 92.5 $mg \cdot cm^{-2}$ for the undoped and doped electrode, respectively. The similar weight gain for these two electrodes indicates that difference caused by the amount of coating deposition should be minor. Thus, the relatively long service life of doped PbO_2 electrodes is possible due to the minimized diffusion of electrolyte through defects into the titanium base, where the oxygen evolution reaction would take place. An insulate TiO_2 layer therefore should be formed between the titanium base and the outer-layer, and this is confirmed by the SEM images that there are less defects on the surface of the doped electrode. For the undoped PbO_2 electrode, defects were formed during the electrochemical decomposition of PbO_2 crystal, and this leads to the inner stress in the PbO_2 layer. However, for the doped electrode, TiO_2 particles would absorb on the defects of the PbO_2 layer and deposit along with PbO_2 crystals. The TiO_2 incorporated PbO_2 structure greatly reduces the inner stress of the original PbO_2 layer, leading to the enhancement of the binding force between the titanium base and the outer oxide layer. This may be the other reason for a longer service life of the doped electrode.

3.4 Linear scanning voltammetry

Linear scanning voltammetry was employed to study the electrochemical and photo-electro chemical behavior of the TiO_2-doped PbO_2 electrode. Fig. 4 shows the results in a 20 $g \cdot L^{-1}$ Na_2SO_4 solution with or without the UV irradiation, where the electrode potential was swept from 0.0 to 2.5 V (vs. Ag/AgCl) at a scan rate of 20 $mV \cdot s^{-1}$.

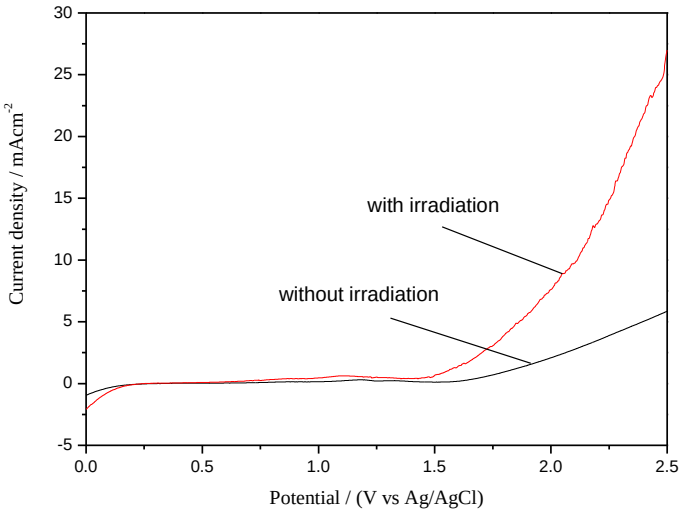

Figure 4. Linear scanning voltammograms of the TiO_2-doped PbO_2 electrode in a 20 $g \cdot L^{-1}$ Na_2SO_4 solution with and without UV irradiation

It was observed that without the irradiation, the doped electrode presents typical electrode characteristics (i.e. voltammogram featureless) from 0.0 to 1.5 V; beyond this range, the oxygen evolution occurs and simultaneously evidenced by a rapid increase in current density. In the presence

of UV illumination, however, the oxygen evolution reaction is shifted towards lower potential. In this study, to generate a 1.0 $mA \cdot cm^{-2}$ current density, the required potential is 1152 and 1810 mV for the cases with or without the irradiation, respectively. Based on the above observation, it was confirmed that the incorporation of TiO_2 particles into the PbO_2 matrix can intensify the photoresponse of PbO_2 electrodes. This result was similar to R. Amadelli's reports [27].

3.5 Photo-electrochemical degradation

3.5.1 Irradiation

Fig. 5 compares the color removal efficiency of methyl orange in water by using the two prepared electrodes with or without the presence of UV illumination, where the involvement of UV always improves the color removal. For the undoped electrode, the removal efficiency increased gradually and reached 77.1% and 74.3% in 120 min with or without the presence of UV, respectively. For the doped electrode without UV, a similar decay pattern was observed with a final removal of 66.4%.

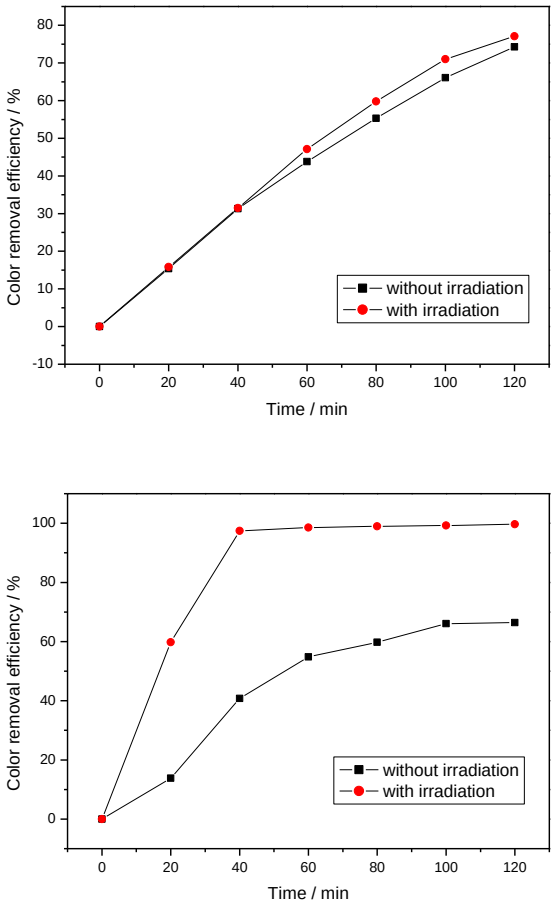

(a) The undoped PbO_2 electrode (b) The doped PbO_2 electrode

Figure 5. Color removal efficiency of two different electrode with ad without irradiation; E_{anode} = 1.5V, pH = 2.5

It should be noted that for the doped electrode with UV, a quick initial removal rate was observed, where 97.4% of the dye was removed in 40 min. This significant rate improvement suggests a good potential of using doped electrode in real application.

To confirm the result of photo-electrochemical degradation, the UV–Vis absorption spectra of each electrode was measured at the range of 250–900 nm as shown in Fig. 6. The undoped electrode had a slight absorbance in the UV region, which explains the increase of dye removal when it is exposed to the irradiation [28]. The TiO_2-doped PbO_2 electrode however has a stronger absorbance in the UV region (< 345 nm) than that of the undoped PbO_2 electrode. This indicates that the incorporation of P25 TiO_2 into the PbO_2 electrode can improve the absorption performance of electrodes in the UV region.

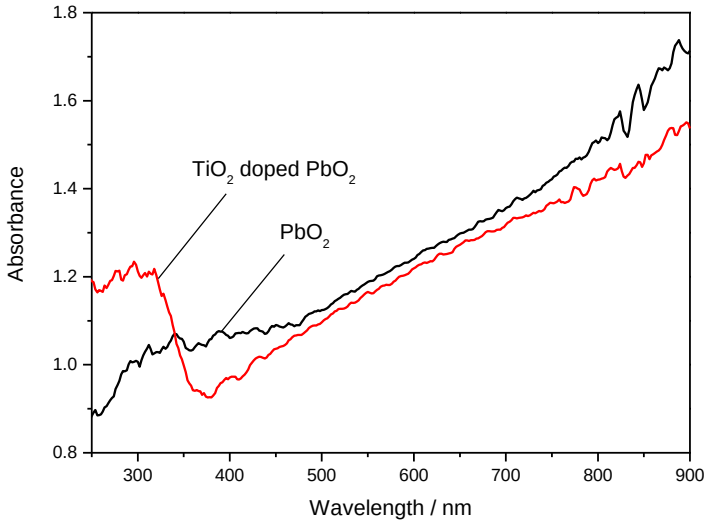

Figure 6. The UV-Vis spectra of the undoped and the TiO_2-doped PbO_2 electrode

3.5.2 Applied potential

The applied potential was found to affect the removal efficiency of the photo-electrochemical degradation process. Fig. 7 shows the degradation results of three different potentials applied on the TiO_2-doped PbO_2 electrode with irradiation. There is no color removal at all when no voltage was applied (0.0 V), indicating the photocatalysis in removing dye is insignificant, especially in the case of small loading amount of TiO_2 catalysts on the electrode. When the applied potential increased to 0.5 and 1.5 V, the color removal degradation reached to 58.1% and 97.2%, respectively, after 2 hours. Undoubtedly, the color removal process was promoted by the increase of applied voltage. According to previous studies [10, 12-15], photogenerated carriers can be effectively separated through the externally applied electric field on a photo-electro anode which drives the electrons migrating to the opposite electrode along the electric gradient. When the applied potential increases (i.e. the drive force increases), the separation of photogenerated carrier (i.e. electrons and holes) become more efficient and leads to the formation of strong oxidants (hydroxyl radicals) in the solution.

It should be noted that for the photo-electro catalytic process, an optimum value of applied potential may be possible. In general, the separation of photogenerated carriers increased as the applied potential increased; when the applied potential is above the optimal voltage, the recombination rate of electrons and holes increased. For example, in electrocatalytic process, the energy consumed may be used to produce oxygen at the anode when the applied voltage is beyond the oxygen evolution potential, in which the degradation of organic matters will be retarded [1].

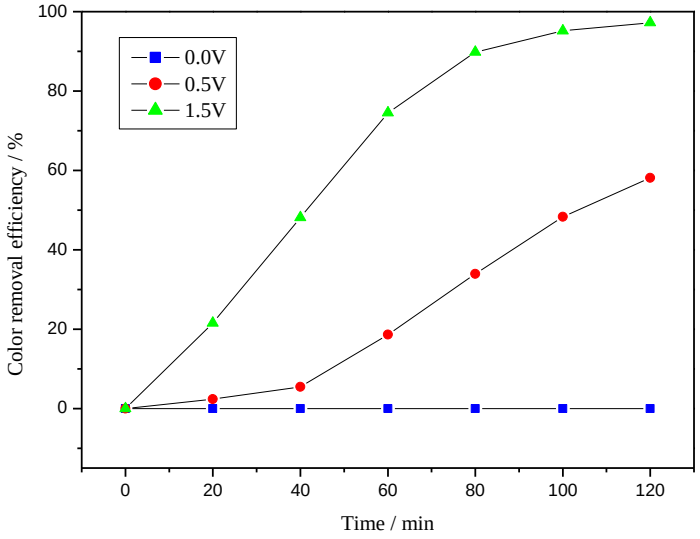

Figure 7. Color removal efficiency under different potentials applied on doped electrode with irradiation; pH = 6.5

3.5.3 Initial pH

The pH level of solution may also introduce an impact on the degradation process, because of the possible change of probe property in molecular level and the alternation of the nature of active site on the electrode surface/electrolyte solution interface. The adsorption of probe on electrode surface is significantly influenced by the above factors, which further affects the follow-up reactions on the electrode surface. So it is necessary to investigate the effect of pH level on color removal.

Fig. 8 shows the color removal efficiency with various initial pH levels using the TiO_2-doped PbO_2 electrode in the presence of light source. The overall removal efficiency of methyl orange at the end of reaction (2 hrs) was 99.6%, 97.2% and 82.3% for the initial pH of 2.5, 6.5 and 11, respectively. The result demonstrates that the lower the initial pH the better the overall removal efficiency and faster to reach that efficiency.

The surface charge of titanium dioxide is mainly determined by the pH value of solution. The isoelectric point (pH_{zpc}) for titanium dioxide is 6.3; when solution pH < pH_{zpc}, the surface of TiO_2 particles is positively charged and it's negatively charged when pH > pH_{zpc}[29]. Since the methyl orange is negetively charged with a sulfonic acid group, it can easy attract to the surface of TiO_2 in acidic solution, which facilitates the degradation of methyl orange. On the contrary, when the pH value

of solution is above the isoelectric point (6.5), the percentage of positive charged TiO_2 surface decreases significantly, which induce a repulsion force between the methyl orange molecules and the TiO_2 surface. This explains the lower removal efficiency in alkaline condition. Under these circumstances, the organic pollutants are likely decomposed mainly by the indirect degradation.

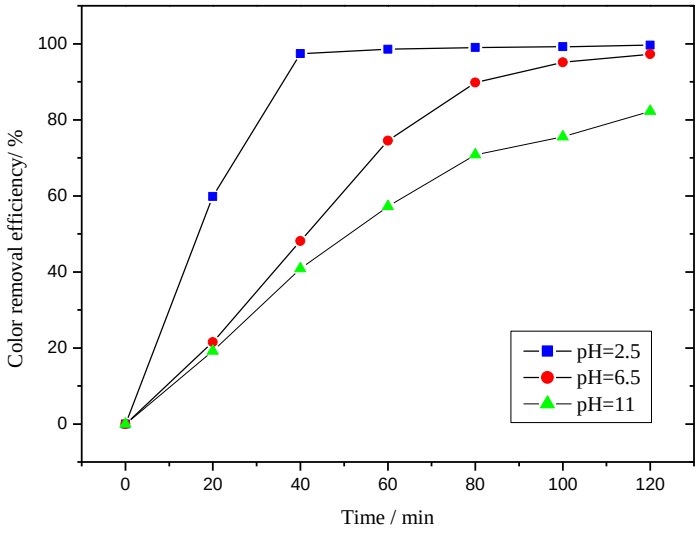

Figure 8. Color removal efficiency for different initial pH value on doped electrode with irradiation; E_{anode} = 1.5 V

3.5.4 P25 amount used in co-deposition solutions

TiO_2 particles play a significant role in enhancing the PbO_2 electrodes' service life and photo response[ ]. Accelerated life test was conducted to investigate the service life of electrodes by varying the dosage in P25-TiO_2 doping. As shown in Fig. 9, it's interesting to note that not all the doped electrodes gained a positive increase in the test. At the loading dosage of P25 at 5 $g \cdot L^{-1}$, the improvement of the lifetime of electrode was optimized (160h). However, further increase or decrease of the dosage leads to a shorten lifetime. The possible reason for this observation is likely because the overdosed P25 in the PbO_2 layer will induce the breakage of PbO_2 layer and reduce the binding force between the outer layer and the inner layer.

Fig. 10 compares the removal efficiency of MO at different doping levels with and without illumination. It was found that, without irradiation, the P25 loading dosage has little effect on the removal efficiency. However, in the presence of light, significant enhancement in treatment efficiency was observed, especially at the P25 loading dosage of 5 $g \cdot L^{-1}$, similar to that in the lifetime test. This result can be attributed to the followings: the TiO_2 particles, as photocatalyst, can absorb UV energy and convert photons to electrons resulting in the synergetic effect in the degradation process. However, TiO_2 is a semiconductor with poor conductive property, the overall conductivity of PbO_2 electrodes is affected by the excessive TiO_2 doping, which results in the negative effect in the degradation.

Experimental results indicate that the TiO_2 dosage of 5 $g \cdot L^{-1}$ is optimal for the TiO_2 doped PbO_2 electrode.

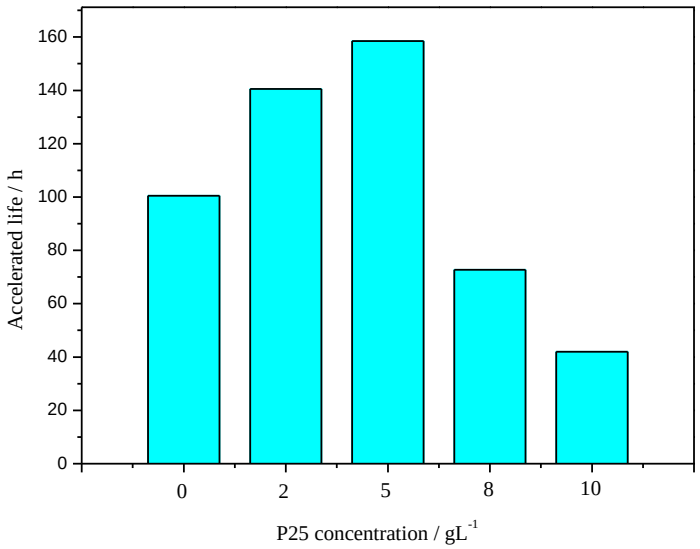

Figure 9. Accelerated life tests of different doped electrodes in 3 $mol \cdot L^{-1}$ H_2SO_4 solution under 1500 $mA \cdot cm^{-2}$

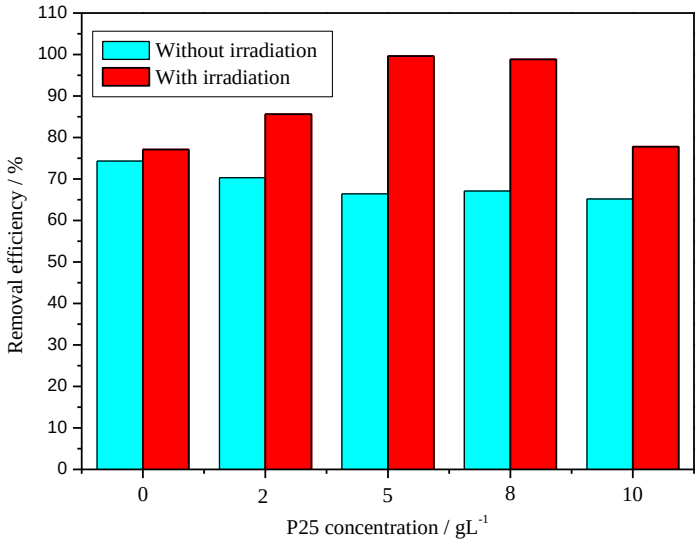

Figure 10. Color removal efficiency for P25 amount used in co-deposition solutions on the doped electrode with the irradiation; E_{anode} = 1.5 V, pH = 2.5

The result of XRF characterization on titanium content in different samples is displayed in Table 1. As we can see, the Pb content does not show much difference among the prepared samples, while there is an apparent change in Sn content. As we mentioned before, the electrode was fabricated on titanium substrate coated with Sb-doped SnO_2 as intermediate layer and PbO_2 as outer layer. In the undoped electrode, electrons penetrated through the PbO_2 and Sb-SnO_2 layers, reaching at the titanium

substrate. Therefore, the detected Sn was relatively high and the Ti content represented the concentration of Ti in titanium substrate. When 2 $g \cdot L^{-1}$ P25 TiO_2 was introduced to the electrode, the TiO_2 particles combined with PbO_2 shielded part of electrons passing through, so the Sn content decreased and the Ti content reflected the actual doping amount of P25 TiO_2. With the enhancement of P25 doping level in Ti/PbO_2 electrodes, the corresponding values of Ti content also show an increase trend from 0.346% in 2 $g \cdot L^{-1}$ P25 doped electrode to 1.62% in 10 $g \cdot L^{-1}$ P25 doped electrode, except that the Ti content in 5 $g \cdot L^{-1}$ P25 doped sample is much similar with that of 8 $g \cdot L^{-1}$ TiO_2 doped electrode. Meanwhile, the Sn content decreases until no Sn content can be detected, it can be interpreted that TiO_2 particles doped in the PbO_2 layer improved the compactness of the original Ti/PbO_2 electrode. Combined with the result of MO degradation test, it is concluded that there exists an optimal TiO_2 doping level to enhance the Ti/PbO_2 photoelectrocatalytical efficiency, which is 5 $g \cdot L^{-1}$ P25 TiO_2 doped electrode.

Table 1. The XRF analysis result of the undoped and doped electrodes

	Pb/%	Sn/%	O/%	C/%	Ti/%	Cl/%	Si/%	Cu/%	F/%
0 $g \cdot L^{-1}$	69.8	5.02	18.6	4.47	0.988	-	-	0.11	0.993
2 $g \cdot L^{-1}$	74.7	0.719	20.7	3.36	0.346	0.0735	0.0751	-	-
5 $g \cdot L^{-1}$	73.1	0.106	22.1	3.94	0.61	0.105	-	-	-
8 $g \cdot L^{-1}$	74.2	-	21.6	3.5	0.53	0.121	-	-	-
10 $g \cdot L^{-1}$	72.9	-	22.3	3.16	1.62	-	-	-	-

4 CONCLUSIONS

In this study, P25 doped PbO_2 electrodes based on the Ti/SnO_2-Sb substrate were fabricated by co-deposition method. XRD and SEM tests were conducted to characterize the electrode's crystal texture and surface morphology. The XRD result shows that the diffraction peak at 25.3° for the doped electrode has an apparent increase which is not available for the undoped electrode. This indicates that P25 particles were successfully doped into the PbO_2 layer through co-deposition. A significant change in morphology is observed through SEM images that the TiO_2 doped PbO_2 electrode has a flawless surface which is beneficial for the stability of electrodes. The service life of electrodes was measured through an accelerated lifetime test, which is doubled for the TiO_2 doped PbO_2 electrode (158h) than that of the undoped electrode (71 h). A significant synergetic effect was observed in the linear scanning voltammetry and the organic degradation tests under irradiation. The color removal efficiency of a 5 $g \cdot L^{-1}$ TiO_2 doped PbO_2 electrode is increased from 66.4% to 99.6% when the irradiation was induced into the reaction system. Acidic condition is preferred for the methyl orange degradation because adsorption between methyl orange molecules and TiO_2 particles is higher. All the doped electrodes with different doping levels show higher removal efficiency under irradiation, compared to that of dark reactions. The electrode was optimized at the TiO_2 doping amount of 5 $g \cdot L^{-1}$, in terms of the accelerated life tests and the organic degradation tests.

ACKNOWLEDGMENTS
The authors gratefully acknowledge the financial support from the Ph. D. Programs Foundation of Ministry of Education of China (20090201110005), the Fundamental Research Funds for the Central University (2011JDHZ36), and the Joint Supervision Project of Hong Kong Polytechnic University (GU-784).

References

1. M. H. Zhou and J. J. He, *J. Hazard. Mater.*, 153 (2008) 357
2. M. Panizza and G. Cerisola, *J. Hazard. Mater.*, 153 (2008) 83
3. M. T. Fukunaga, J. R. Guimaraes and R. Bertazzoli, *Chem. Eng. J.*, 136 (2008) 236
4. C. A. Martinez-Huitle and S. Ferro, *Chem. Soc. Rev.*, 35 (2006) 1324
5. M. Muruganandham and M. Swaminathan, *Dyes and Pigments*, 62 (2004) 269
6. Rauf M A and Salman Ashraf S, *Chem. Eng. J.*, 151 (2009) 10
7. U. G. Akpan and B. H. Hameed, *J. Hazard. Mater.*, 170 (2009) 520
8. X. H. Li, D. Pletcher and F. C. Walsh, *Chem. Soc. Rev.*, 40 (2011) 3879
9. R. Davide, D. Daniele, F. Maurizio and A. Angelo, *Chem. Soc. Rev.*, 38 (2009) 1999
10. K. Vinodgopal, S. Hotchandani and V. K. Prashant, *J. Phys. Chem.*, 97 (1993) 9040
11. S. J. Tarek, Y. G. Montaser, E. E. Ibrahim, R. S. and A. N. Rabab, *J. Hazard. Mater.*, 185 (2011) 353
12. C. M. Fan, B. Hua, Y. Wang, Z. H. Liang, X. G. Hao, S. B. Liu and Y. P. Sun, *Desalination*, 249 (2009) 736
13. M. Tian, A. Brian, J. L. Wen, R. M. Asmussen and A. C. Chen, *Electrochimica Acta*, 54 (2009) 3799
14. G. T. Li, J.H. Qu, X. W. Zhang and J. T. Ge, *Water Research*, 40 (2006) 213
15. R. T. Pelegrini, R. S. Freire, N. Duran and R. Bertazzoli, *Environ. Sci. Tech.*, 35 (2001) 2849
16. J. T. Kong, S. Y. Shi, L. C. Kong, X. P. Zhu and J. R. Ni, *Electrochimica Acta*, 53 (2007) 2048
17. X. H. Mao, F. Tian, F. X. Gan, A. Lin and X. J. Zhang, *Rus. J. Electrochem.*, 44 (2008) 865
18. Y. Q. Wang, H. Y. Tong and W. L. Xu, *Rare Met. Mater. Eng.*, 33 (2004) 976
19. S. P. Tong, C. A. Ma and H. Feng, *Electrochimica Acta*, 53 (2008) 3002
20. A. M. Polcaro, S. Palmas, F. Renoldi and M. Mascia, *J. Appl. Electrochem.*, 29 (1999) 147
21. P. Marco and C. Giacomo, *Ind. Eng. Chem. Res.*, 47 (2008) 6816
22. I. Sires, B. Enric, C. Giacomo and P. Marco, *J. Electroanaly. Chem.*, 613 (2008) 151
23. G. T. Li, J. H. Qu, X. W. Zhang, H. J. Liu and H. N. Liu, *J. Mol. Cataly. A: Chem.*, 259 (2006) 238
24. G. T. Li, J. H. Qu and R. C. Wu, *Chinese Science Bulletin*, 50 (2005) 1185
25. P. Q. Li, G. H. Zhao and X. Cui, *J. Phys. Chem. C*, 113 (2009) 2375
26. Y. W. Yao, C. M. Zhao and J. Zhu, *Electrochimica Acta*, 69 (2012) 146
27. R. Amadelli, L. Samiolo, A. B. Velichenko, V. A. Knysh, T. V. Lukyanenko and F. I. Danilov, *Electrochimica Acta*, 54 (2009) 5239
28. G. T. Li, H. Y. Yip, K. H. Wong, C. Hu, J. H. Qu, and P. K. Wong, *J. Environ. Sci.*, 23 (2011) 998
29. A. Fujishima, X. T. Zhang and A. D. Tryk, *Surf. Sci. Rep.*, 63 (2008) 515